TGBA and TGBC phases in some chiral tolan derivatives

H. Nguyen, A. Bouchta, L. Navailles, P. Barois, N. Isaert, R. Twieg, A. Maaroufi, C. Destrade

Classification
Physics Abstracts
64.70M

TGB_A and TGB_C phases in some chiral tolan derivatives

H. T. Nguyen ([1]), A. Bouchta ([1], *), L. Navailles ([1]), P. Barois ([1]), N. Isaert ([2]), R. J. Twieg ([3]), A. Maaroufi ([4]) and C. Destrade ([1])

([1]) Centre de Recherche Paul Pascal, Avenue A. Schweitzer, F-33600 Pessac Cedex, France
([2]) Laboratoire de Dynamique et Structure des Matériaux Moléculaires (U.R.A., CNRS n 801), Université de Lille 1, U.F.R. de Physique, F-59655 Villeneuve d'Ascq Cedex, France
([3]) IBM Almaden Research Center, 650 Harry Road, San Jose, CA 95120-6099, U.S.A.
([4]) Université de Tetouan, Département de Chimie, B.P. 5204, Tetouan, Morocco

(*Received 13 May 1992, accepted 30 June 1992*)

Résumé. — Trois produits (n = 10, 11, 12) de la série chirale : 3-fluoro-4-[(R) ou (S)-1-methylheptyloxy]-4'-(4"-alcoxy-2", 3"-difluorobenzoyloxy) tolanes ($nF_2BTFO_1M_7$) ont été synthétisés. Les deux premiers produits présentent la phase S_A^* hélicoïdale ou torse (TGB_A). L'existence de la nouvelle phase TGB_C, prédite par Renn et Lubensky, a été trouvée dans les deux derniers matériaux et prouvée par plusieurs études : observation microscopique, AED, méthode de contact, mélanges binaires, diffraction de rayons X et mesures du pas d'hélice. Le diagramme de phase réalisé entre ces trois matériaux est similaire à celui prédit par Renn. Les propriétés électrooptiques de la phase S_C^* ferroélectrique ont aussi été étudiées.

Abstract. — Three chiral compounds (n = 10, 11, 12) belonging to the optically active series : 3-fluoro-4-[(R) or (S)-1-methylheptyloxy]-4'-(4"-alkoxy-2", 3"-difluorobenzoyloxy) tolans ($nF_2BTFO_1M_7$) have been synthesized. The helical S_A^* phase or TGB_A phase is found in the decyloxy derivative. The most interesting compound is obtained with n = 11. It displays, for the first time, two TGB phases (TGB_A and TGB_C phases). The nature of these helical smectic phases is confirmed by different studies : optical observation, DSC, contact method, mixtures, X-ray diffraction and helical pitch measurements. The electrooptical properties of the S_C^* phase have also been studied.

1. Introduction.

The discovery of the new helical smectic A* phase or twist grain boundary A phase (TGB_A phase) by Goodby *et al.* [1] in 1989 stimulated the search of such new types of materials. As a matter of fact, in the last three years, there has been an effort by several groups [1-13] to understand the effect of chirality on smectic A (S_A) liquid crystals. This work began with the prediction by Renn and Lubensky [4] of the existence of a new highly

(*) *Permanent address :* Université de Tetouan, Département de Chimie, B.P. 5204 Tetouan, Maroc.

dislocated smectic A phase called TGB_A phase in chiral systems. This prediction is based on the de Gennes model [14] which established a strong analogy between the nematic-smectic A ($N - S_A$) transition and the normal-superconductor transition in metals.

Recently Renn and Lubensky [5] and Renn [15] predicted the existence of tilted twist grain boundary phases : the so-called TGB_C (Fig. 1) and TGB_C^* phases within a chiral extension of the Chen Lubensky [16] model of a NAC point. They consist of a twisted array of two dimensional smectic slabs, stacked along the pitch axis. The three phases are distinguished by the nature of the slabs : TGB_A, TGB_C and TGB_C^* consist of S_A, smectic C (S_C) and chiral smectic C (S_C^*) slabs respectively. The TGB_A phase is found and identified in several systems and with different phases sequences : I-TGB_A-S_C^*-K, I-BP-N*-TGB_A-S_A, I-BP-N*-TGB_A-S_A-S_C^* and I-BP-N*-TGB_A-S_C^* whereas the TGB_C and TGB_C^* structures are not yet known (I, BP, N* and K stand for isotropic, blue phase, cholesteric and crystal respectively).

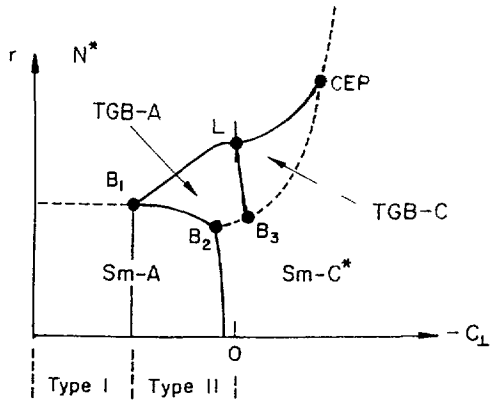

Fig. 1. — Theoretical phase diagram proposed by Renn in the case of splay and twist constants (K_1 and K_3) lower than the bend rigidity K_1 (reproduced from Ref. [15], courtesy of S. Renn). Two twist grain boundary smectic phases are predicted instead of a simple NAC point in a chiral Chen-Lubensky model [19].

We have reported in four different chiral tolan series [9, 10], the existence of TGB phases obtained with very long chains (C_{18} for example) and measured layer spacings (d) significantly shorter than the molecular length (ℓ) (for example, d and ℓ are respectively 44.1 Å and 56.2 Å for the TGB phase of compound $18FBTCO_1M_7$) [9]. We suspected at first that this phase could be a TGB_C phase but subsequent studies with different techniques (racemic mixture, contact method, X-ray diffraction, light reflectivity) indicated a TGB_A phase instead. We now report the discovery of the TGB_C phase in new series having the general formula :

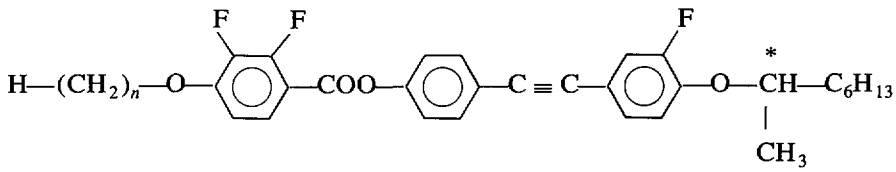

$nF_2BTFO_1M_7$

where n = 10, 11 and 12.

The paper is organized as follows : the chemical synthesis of the material is briefly presented in section 2. Section 3 is devoted to the mesomorphic properties of the three pure homologs n = 10, 11 and 12 of the series. Microscopic observations and calorimetric studies are presented. The properties of various mixtures are reported in section 4. The effect of molecular chirality is investigated in (R) and (S) enantiomer mixtures (including racemic). Miscibility with other compounds of identified structure (TGB$_A$) is studied. Finally, binary phase diagrams of optically pure homologs (n = 10, n = 11) and (n = 11, n = 12) are obtained from careful DSC data. The topology of the experimental phase diagram is found to be strikingly similar to the theoretical phase diagram (Fig. 1) which exhibits two different twisted grain boundary smectic phases TGB$_A$ and TGB$_C$. X-ray diffraction studies are reported in section 5 and optical pitch measurements in section 6. Electrooptical properties (i.e. polarization and tilt angle measurements) on the S_C^* phase of the n = 12 homolog are given in section 7. Section 8 is devoted a discussion of the influence of molecular architecture on the existence of helical smectic phases. Our results are finally summarized in the conclusion.

2. Synthesis.

The three compounds were prepared following the reaction :

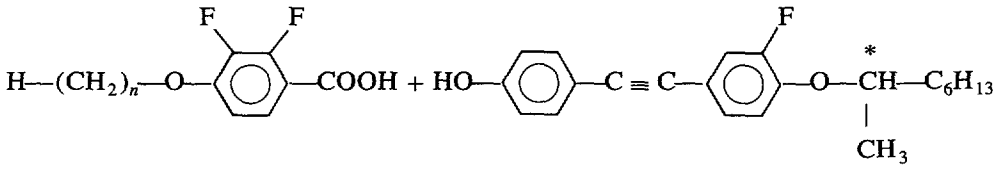

1 2

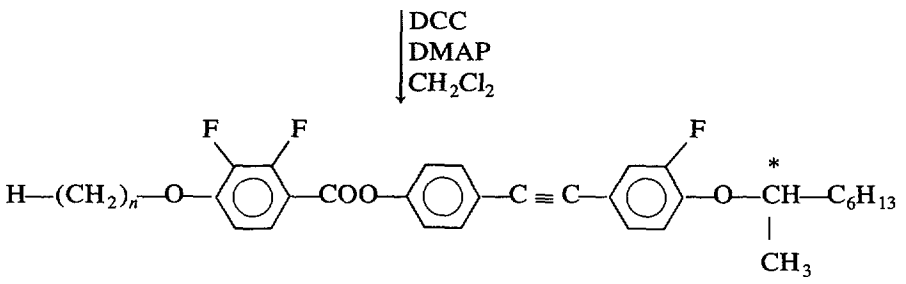

3

nF$_2$BTFO$_1$M$_7$.

The 4-alkoxy-2,3-difluorobenzoic acids are prepared following the well known method [17]. The synthesis of (R) and (S)-3-fluoro-4-(1-methylheptyloxy)-4'-hydroxytolan is described in a previous paper [10]. The final compounds 3 (nF$_2$BTFO$_1$M$_7$) were obtained by esterification reaction with dicyclohexyl carbodiimid (DCC) as dehydrating agent. They were purified by chromatography over silica gel using toluene as eluent and recrystallized in absolute ethanol. They give satisfactory elemental analysis.

3. Mesomorphic properties.

The phase assignments and corresponding transition temperatures were determined by thermal optical microscopy using a Zeiss Universal Polarizing light microscope equipped with

a Mettler FP52 microfurnace and FP5 control unit and by differential scanning calorimetry (Perkin Elmer 7). The liquid crystal transition temperatures and enthalpies of these new materials are presented in table I.

Table I. — *Transition temperatures* (°) *and enthalpies in italic* ($J.g^{-1}$) *of compounds* $nF_2BTFO_1M_7$.

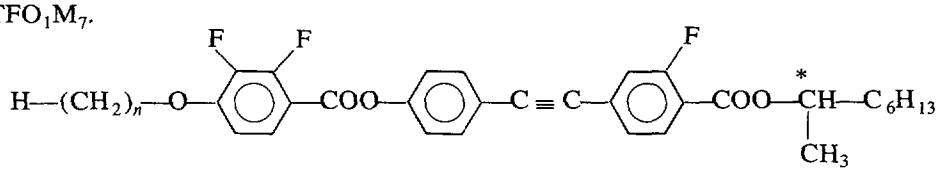

n	K	S_C^*	S_X^*	S_A^*	N*	BP	I
10	• 59.1	• 98.4	—	• 105.8	• 114.5	• 115.7	•
	54.1	~ 0		*0.88*	*1.84**		
11	• 46.4	• 100.6	• 101.3	• 104.2	• 111.9	• 112.7	•
	68.9	*0.17**			~ 0 *1.9**		
12	• 36.6	• 102.8	• 103	—	• 110.5	• 111.7	•
	63.1	*0.4**			*1.8**		

The meanings of the signs used in this table are :

K crystalline phase ; I : isotropic phase ; N* : cholesteric phase ; BP : blue phases ; S : smectic phases A*, C*, X* smectic phases S_A^*, S_C^*, S_X^* ;

• the phase exists ; — the phase does not exist ;

* the sum of two or the three transition enthalpies : BP-I and N*-BP or S_C^* – S_X^* and S_X^*-S_A^* or S_C^*-S_X^* and S_X^*-N*

3.1 MICROSCOPIC OBSERVATIONS. — These three compounds give three different phase sequences : K-S_C^*-S_A^*-N*-BP-I, K-S_C^*-S_X^*-S_A^*-N*-BP-I and K-S_C^*-S_X^*-N*-BP-I. On cooling from the isotropic liquid they all exhibit blue phases. The transition from isotropic liquid to blue phase III was not easily observed in the microscope but the BP III → BP II and BP II → BP I transitions are clearly detected on cooling. Blue phase II is obtained with a characteristic iridescent defect texture and on further cooling, blue phase I appears as a grazed platelet texture. The cholesteric phase has two typical textures : fan shaped and Grandjean plane textures. Now on further slow cooling from the N* phase of the decyloxy derivative ($10\ F_2BTFO_1M_7$), the N* S_A^* transition occurs and the helical S_A^* phase is characterized by another Grandjean plane texture or vermis texture. Anticipating X-ray and pitch measurements data (Sects. 5 and 6), we identify this helical smectic A phase (S_A^*) with the TGB_A structure proposed by Renn and Lubensky [4]. When the helical S_A^* transforms into a S_C^* phase one can observe several dechiralization lines at the transition and then in S_C^* phase, classical striated fan shaped or pseudo-homeotropic texture. The N*-S_A^* transition is also observed in the undecyloxy member ($11\ F_2BTFO_1M_7$) but on cooling from the helical S_A^* phase (or TGB_A phase), another Grandjean plane texture and pseudo homeotropic texture appears. This phase is also a helical smectic phase the helix axis of which is parallel to the layers as in the case of N* and TGB_A phases. This unknown chiral phase that we denote S_X^* for the moment has a very short temperature range (0.7 °C) between TGB_A and ferroelectric S_C^* phases. It is also present in the dodecyloxy derivative ($12\ F_2BTFO_1M_7$) with 0.4 °C temperature range between N* and S_C^* phases whereas in this compound, the TGB_A phase disappears. In order to confirm the nature of the TGB_A phase and characterize the « structure » of the S_X^* phase we

used different complementary techniques : DSC, racemic mixtures, contact method, X-ray diffraction and pitch measurement.

3.2 CALORIMETRIC STUDIES. — Transition enthalpies were determined by differential scanning calorimetry (DSC, Perkin Elmer 7), and are given in table I. We must point out that only the melting transition enthalpies are easy to determine separately, the other transitions are either too small (S_C^*-S_A^* and S_A^*-N* transitions) or very close together (N*-BP and BP-I or S_C^*-S_X^* and S_X^*-S_A^* .). In the latter case, it is very difficult to obtain separate transition enthalpies and we give the sum of them. The existence of the S_A^* and S_X^* phases is given in evidence by three thermograms (Figs. 2a, b, c) for heating rates of 0.5 °C mn^{-1} In this figure only the transitions near the clearing point are given. It shows clearly different phase transition I-BP II, BP II-BP I, BP I-N*. In figure 2a, the N*-S_A^* transition is characterized by a flat peak as observed in the *n*FBTFO$_1$M$_7^{10}$. This peak flattens out with the undecyloxy derivative. Figure 2b shows also two peaks which are very close together and partially overlap. They correspond to the S_C^* to S_X^* and S_X^* to S_A^* transitions. They are also found in dodecyloxy derivative (Fig. 2c), but in the latter case, they correspond instead to the S_C^* to S_X^* and S_X^* to N* transitions since the helical S_A^* disappears in the n = 12 compound.

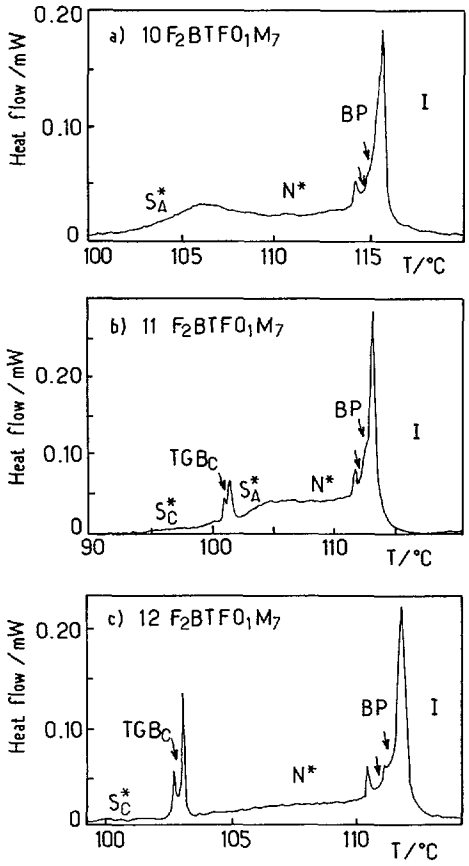

Fig. 2. — Differential scanning calorimetry thermogram for heating cycle of *n*F$_2$BTFO$_1$M$_7$. Heating rate = 0.5 °C.mn^{-1} (a) n = 10 ; (b) n = 11 ; (c) n = 12.

4. Mixture studies.

4.1 RACEMIC MIXTURES. — Table II gives the transition temperatures and enthalpies of the three racemic compounds nF$_2$BTFO$_1$M$_7$. It shows clearly that :

- the achiral phase between N and S_C of $n = 10$ member is a smectic A phase ;
- the smectic S_X^* phase is not a S_A^* phase (in Slaney's compounds [8] and in the nFBTFO$_1$M$_7$ series [10] the phase sequence K-S_C^*-S_A-S_A^*-N*-BP-I is often observed) because the racemic dodecyloxy derivative only displays two phases : S_C and N. So S_X^* is presumably a chiral tilted S_C phase ;
- we must point out that the clearing points of the racemic or the enantiomeric compounds are the same. This behaviour is also observed with S_A-N compared to S_A^*-N* or S_C-N(S_X^*-N*). This observation suggests that the clearing points, S_A-N and S_C-N transitions are not too much influenced by the degree of molecular chirality. This behaviour is confirmed by optical purity studies.

Table II. — *Transition temperatures* (°) *and enthalpies in italic* (J.g^{-1}) *of compounds* nF$_2$BTFO$_1$M$_7$.

n	K	S_C	S_A	N	I
10	• 73	• 98.8 ~ 0	• 106 1.0	• 115.9 *1.8*	•
11	• 76	• 102.4 *0.1*	• 104 *1.0*	• 113.2 *1.8*	•
12	• 76	• 103.5 *0.28*	—	• 111.8 *2.9*	•

4.2 OPTICAL PURITY STUDIES. — The dependence of the existence of the helical S_A^* phase on optical purity was performed by Slaney *et al.* Here we study the influence of the optical purity on the formation of S_X^* by preparing various mixtures of (R) and (S)-12 F$_2$BTFO$_1$M$_7$. Figure 3 shows a classical behaviour of two enantiomer mixtures. The temperature range of blue phases slightly decreases with decreasing optical purity and the clearing point first decreases, then comes to a minimum which corresponds to the vanishing of the blue phases stability and finally reaches a slight maximum for the racemic mixture. A similar behaviour is observed for the S_X^* existence. The stability of the blue phase and of the S_X^* phase turns out to be strongly dependent on the optical purity just like the helical S_A^* phase. Neither blue phases nor S_X^* are observed beyond a ratio of (70 : 30) of each enantiomer. The clearing point and the N-S_C or N*-S_X^* transition temperature behave the same way with decreasing optical purity. From this point of view, S_A^* and S_X^* exhibit a similar behaviour.

4.3 MISCIBILITY STUDIES. — The nature of the helical S_A^* phase of 10 F$_2$BTFO$_1$M$_7$ is inferred from the miscibility phase diagram (Fig. 4) between (R)-10 F$_2$BTFO$_1$M$_7$ and (R)-11 FBTFO$_1$M$_7$ with the formula and phase sequence [10] :

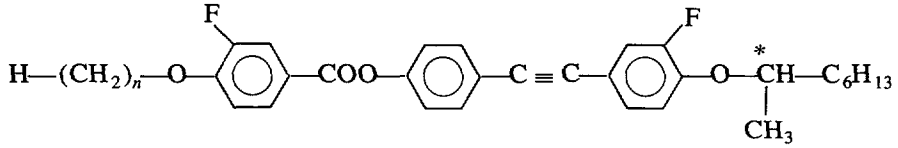

K 68 S_C^* 97.4 S_A^* 100.5 N* 103.5 BP 103.7 I.

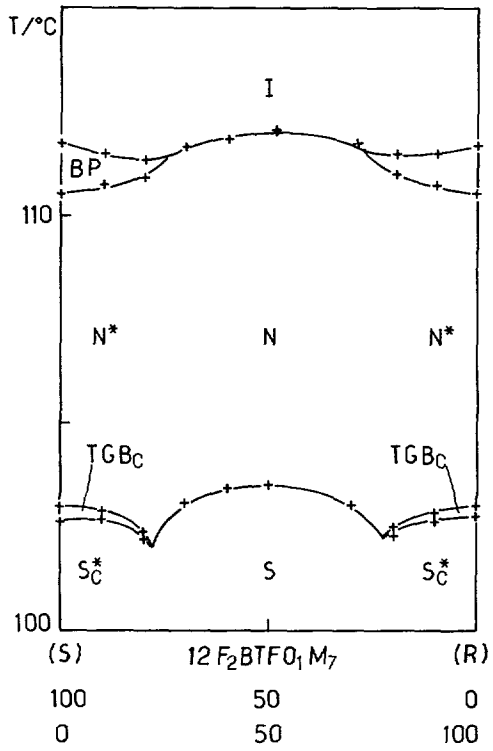

Fig. 3. — Binary phase diagram between (R) and (S) optically active 12 $F_2BTFO_1M_7$.

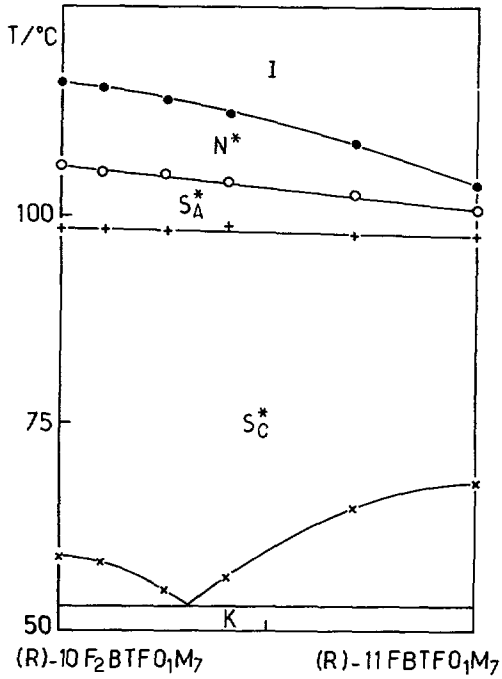

Fig. 4. — Miscibility phase diagram of binary mixtures (wt %) between (R)-10 $F_2BTFO_1M_7$ and (R)-11 $F_2BTFO_1M_7$.

In this study the miscibility of the S_C^* S_A^* and N* phases of these materials is complete and the phase diagram shows thermodynamic ideality. It also proves that the helix of the S_A^* phase of (R)-10 $F_2BTFO_1M_7$ is left-handed.

On the other hand, in order to study the miscibility of the helical S_A^* phase of 10 and 11 $F_2BTFO_1M_7$ and the S_X^* phase of 11 and 12 $F_2BTFO_1M_7$ a phase diagram was obtained by studying the phase transitions in various mixtures (Fig. 5). It is remarkably similar to the theoretical diagram of Renn [15] (Fig. 1) if, anticipating the conclusion of the present paper, S_A^* and S_X^* are identified with TGB_A and TGB_C phases respectively.

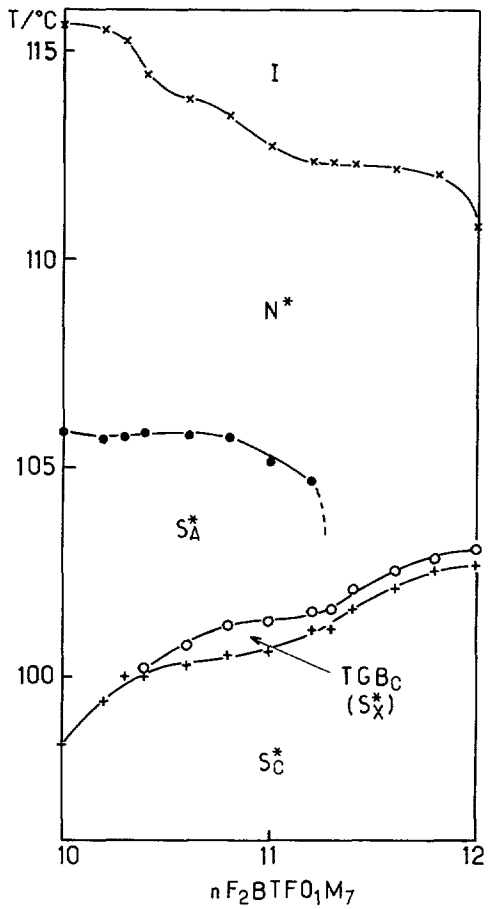

Fig. 5. — Juxtaposition of two binary phase diagrams between (S)-10 and (S)-11 $F_2BTFO_1M_7$ and between (S)-11 and (S)-12 $F_2BTFO_1M_7$.

5. X-ray scattering.

X-ray diffraction is the most appropriate technique to probe the existence of long range smectic order in twist grain boundary phases [1-3].

An average tilt of the molecules with respect to the layers normal however is not so easy to demonstrate. In a conventional smectic C phase, the finite angle between the layers normal and the director **n** can be measured on an oriented sample. Due to the helical twist of the

director, such a characterization is not possible in the TGB$_C$ phase. The existence of a tilt angle θ can however be inferred from the variations of the layer spacing with temperature as we shall see now.

Powder (i.e. non oriented) samples were prepared in 1 mm-diameter Lindemann capillaries with the $n = 10$, $n = 11$ and $n = 12$ homologs. The samples were mounted on a $\theta - 2\theta$ goniometer. The temperature was controlled within a 0.1 °C accuracy. X-ray scattering experiments were performed using Cu Kα radiation from an 18 kW rotating anode X-ray generator. Two different X-ray optics were used :

(i) a high resolution (HR) configuration allowed accurate measurement of the scattering wavevectors : two identical channel cut (3 bounce) germanium (III) crystals were mounted as monochromator and analyzer. The beam size on the sample was 0.8×5 mm^2. The resulting intensity was about 2.5×10^6 photons/s. The resolution was 6.2×10^{-4} Å^{-1} FWHM in the horizontal plane. The scattered profiles were fitted with the actual resolution function obtained by convolution with the vertical resolution (2.55×10^{-2} Å^{-1} FWHM).

Since, our resolution function is not sharp enough to probe the Landau-Peierls effect in the smectic phases, we do not distinguish quasi long range order from true long range smectic order ;

(ii) a low resolution (LR) but high flux configuration was used whenever the scattering intensity was too low to allow reliable HR scans. A flat pyrolytic graphite (002) monochromator delivered a 0.5×2 mm^2 beam onto the sample. The scattered radiation was analyzed by 0.5 mm slits. The resolution was then 2×10^{-3} Å^{-1} FWHM in the scan direction.

Figure 6 shows a HR scattering curve in the S_C^* phase. The peak position q_0 gives the periodicity $d = 2\pi/q_0$ of the smectic order. The variations of the layer spacing d with temperature for the $n = 10$, $n = 11$ and $n = 12$ homologs are plotted in figure 7.

The results of the HR study of the nF$_2$BTFO$_1$M$_7$ series ($n = 10, 11, 12$) are reported below.

• Upon cooling the $n = 10$ homolog from the cholesteric phase, the bragg peaks become resolution limited below 102 °C i.e. at the cholesteric-S_A^* transition. In the meantime, the layer spacing exhibits a continuous increase from 37.6 Å in the cholesteric phase at 106 °C to

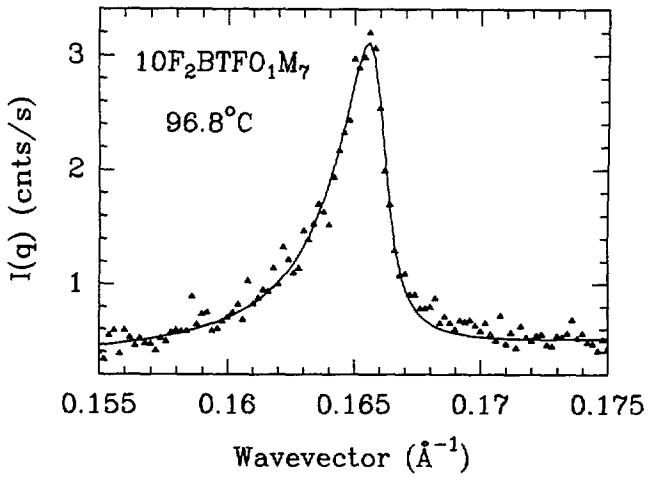

Fig. 6. — High resolution X-ray scan in the S_C^* phase of 10 F$_2$BTFO$_1$M$_7$. The solid line is a fit with the instrumental resolution function. The horizontal resolution given by two channel cut Ge(III) crystals is 6.2×10^{-4} Å^{-1} FWHM whereas the vertical resolution (2.55×10^{-2} Å^{-1} FWHM) is determined by 5 mm slits.

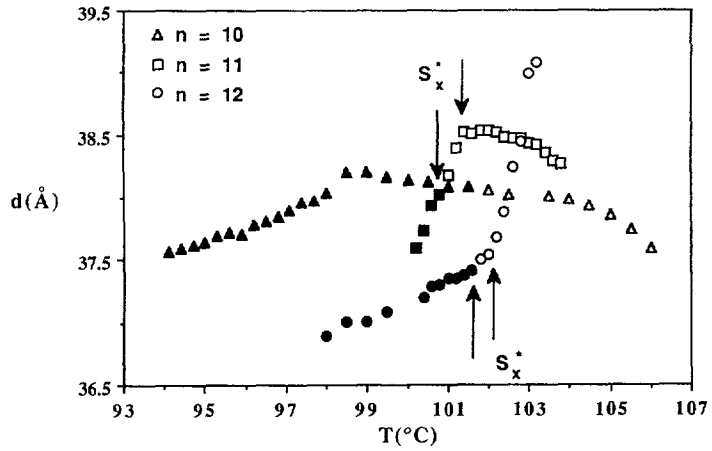

Fig. 7. — Layer spacing *versus* temperature as obtained from X-ray scans for the three homologs of the $nF_2BTFO_1M_7$ series. Triangles correspond to $n = 10$, squares to $n = 11$ and circles to $n = 12$. Full symbols indicate resolution limited peaks (6.2×10^{-4} Å^{-1} FWHM). The arrows show the limits of the S_X^* (or TGB_C) phase in the $n = 11$ and $n = 12$ homologs.

38.2 Å in the TGB_A phase at 98.5 °C. This behaviour can be attributed to a reduction of the interpenetration of the alkyl chains upon cooling. Note that all the measured values are shorter than the length of a molecule in its most extended configuration, 45.4 Å.

Below 98.5 °C, the layer spacings falls off sharply as the tilt of the director relative to the layers normal develops in the chiral smectic C phases (S_C^*).

• The undecyloxy homolog ($n = 11$) exhibits a cholesteric mesophase with short range smectic order. Then upon cooling down to the S_A^* domain the Bragg peaks sharpen up to 4×10^{-3} Å^{-1} (FWHM) which is still about seven times larger than the instrumental resolution. The peaks are well fitted with a Lorentzian (i.e. symmetrical) profile despite the very broad vertical resolution. The layer spacing increases slightly upon cooling just like the decyloxy derivative (Fig. 7). Below 101.4 °C as the new S_X^* phase appears, the layer spacing falls off sharply, indicating a local tilted smectic C order. The width of the Bragg peaks immediately below 101.4 °C is still quite large (5×10^{-3} Å^{-1}). Finally, below 100.8 °C asymetrical resolution limited (6.2×10^{-4} Å^{-1} FWHM) peaks are recovered in the S_C^* phase.

The S_X^*-S_C^* transition is not visible on the plots of figure 7 (layer spacing *vs.* temperature) which shows that the tilt angle behaves continuously and regularly across this transition.

• The tilted nature of the S_X^* phase is more obvious with the third homolog (Fig. 7). Upon cooling the $n = 12$ compound, the layer spacing falls off monotonically, all the way from the cholesteric phase (103.2 °C) to S_C^* (98 °C). Above 102 °C, in the cholesteric phase the width of the observed peaks is clearly larger than the resolution function and continuously decreasing upon cooling. The variation of the layer spacing with temperature is extremely steep ($\Delta d(T)/\Delta T > 1.6$ Å per °C) showing a quickly growing tilt (i.e. a short range smectic C order). As the new S_X^* phase is reached (below 102 °C), the slope $\Delta d(T)/\Delta T$ gets lower. The peaks become almost resolution limited (1×10^{-3} Å^{-1} FWHM) indicating a smectic correlation length larger than 6 000 Å.

Then below 101.6° the S_X^*-S_C^* transition is almost invisible : once again the layer spacing behaves continuously and regularly. The only noticeable difference is that the peaks become truly resolution limited (6.2×10^{-4} Å^{-1} FWHM). Note that the layer spacing is shorter in the

S_X^* phase of the $n = 12$ homolog than in the untilted S_A^* phases of the $n = 10$ and $n = 11$ compounds at the same temperature which again supports the argument of a tilted smectic order.

At this stage, we believe that the existence of a local smectic C order in the S_X^* phase is well established. The broadening of the Bragg peaks, especially with the undecyloxy derivative, has however to be clarified.

Low resolution (LR) scans reveal an asymmetric scattering profile with reinforced high q side of the peaks (Fig. 8) in the S_A^* and S_X^* phases of the three compounds. Two reasons can be invoked to explain this asymmetry : local tilt fluctuations in the vicinity of a smectic A-smectic C transition and/or anisotropic in plane correlation lengths associated with a twist grain boundary structure. As argued by Renn and Lubensky [4] and experimentally shown by Strajer *et al.* [3] the structure factor of an infinite TGB smectic sample exhibits a Gaussian profile $e^{-q_x^2 \xi^2}$ along the pitch direction x of characteristic width $\xi^{-1} \approx 2\ \pi/(\lambda_{c2}\ d)^{1/2}$ where λ_{c2} is the cholesteric pitch at the cholesteric-TGB$_A$ transition. Angular averaging of this structure factor to describe a powder sample produces the asymmetrical profile of figure 8.

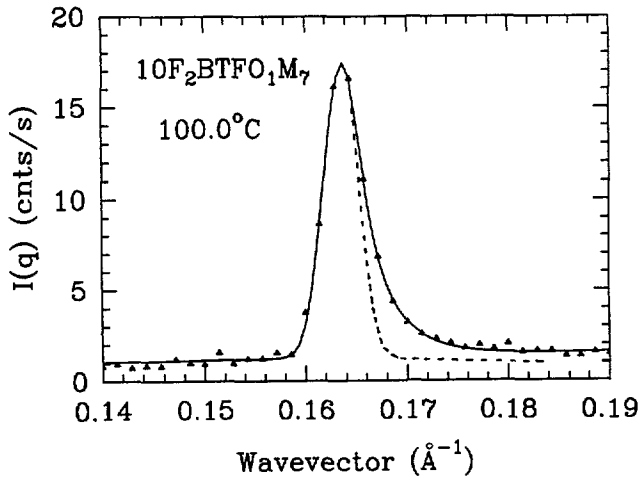

Fig. 8. — Low resolution X-ray scan obtained in the TGB$_A$ phase of 10 F_2BTFO$_1$M$_7$ (powder sample). Solid line is a fit with the theoretical TGB$_A$ structure factor proposed by Renn and Lubensky [4]. The dashed line is the instrumental resolution. The characteristic width of the Gaussian distribution along the pitch axis is about 0.028 Å^{-1}, whereas the calculated value (from Ref. [4] and pitch measurements, Sect. 6) is about 0.010 Å^{-1} This discrepancy may be due to important smectic C fluctuations.

A fit of this LR profile with the TGB structure factor only (i.e. incorrectly neglecting smectic C fluctuations) gives an estimate of $\xi^{-1} \approx 0.028$ Å^{-1} in the S_A^* phase of the $n = 10$ homolog larger than the theoretical estimate $\xi^{-1} \approx 2\ \pi/(\lambda_{c2}\ d)^{1/2} \approx 0.010$ Å^{-1} which suggests that tilt fluctuations are important. These fluctuations are expected to be strongest at the TGB$_A$-TGB$_C$ transition : the broadening of the peaks is indeed found to be maximum at the S_A^*-S_X^* transition on the $n = 11$ homolog.

X-ray experiments on oriented samples are, however, clearly required to distinguish smectic C fluctuations from TGB structure factor effects.

6. Helical pitch measurements.

Most of the twist measurements are performed as previously reported [9, 10] on prismatic samples between very clean rubbed glass plates forming a weak angle (0.25°). An excellent planar orientation is generally achieved with regular Grandjean-Cano steps allowing helical pitch measurement. The rotatory power can also be studied ; its sign gives the helix sense, its value allows to obtain or to confirm the pitch value. In very flat drops, a pseudohomeotropic orientation is generally obtained with in the TGB phase highly packed filaments, the width of which allows an estimation of the pitch.

Figure 9a gives the pitch variation *versus* temperature for 10 $F_2BTFO_1M_7$. Very short below the I-N* transtion (0.22 μm, giving violet selective refraction), the pitch regularly grows up to

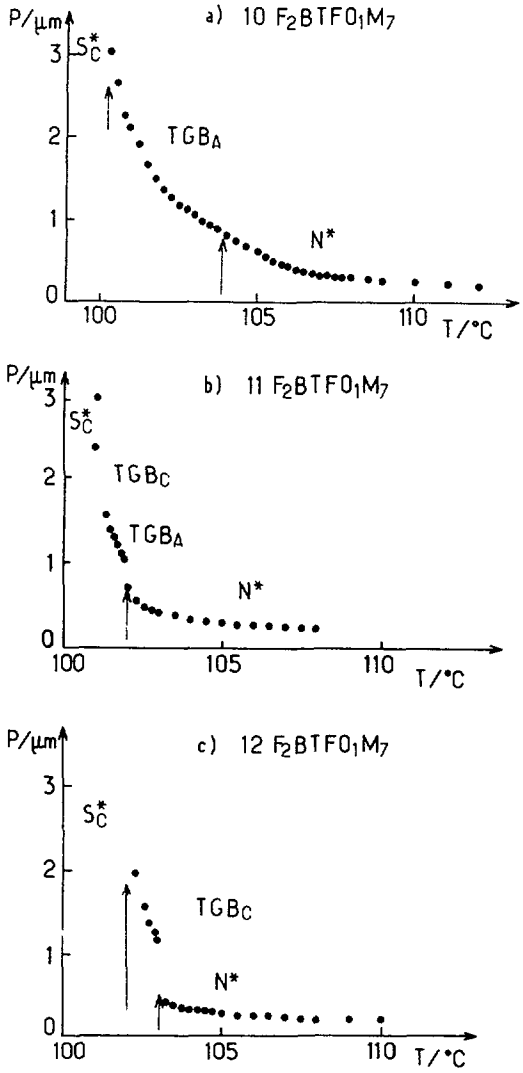

Fig. 9. — Helical pitch variations of $nF_2BTFO_1M_7$. (a) $n = 10$; (b) $n = 11$; (c) $n = 12$.

3-4 μm on cooling ; there is no evidence of singularity at the N*-TGB$_A$ transition. Below 100 °C accurate measurements are not possible since the very high viscosity of the TGB$_A$ phase prevents an easy motion of the Grandjean Cano threads : the TGB$_A$-S$_C^*$ transition occurs at about 99 °C while the twist still remains. With homeotropic drops it is possible to observe a more important divergence of the pitch measuring the width of the filaments just before they get shorter or disappear in the homeotropic S$_C^*$ phase : the observed pitch grows up to 9-10 μm at the transition TGB$_A$-S$_C^*$. This is not of course an intrinsic value considering the importance of surface and thickness effects.

Moreover, these homeotropic drops deposited on rubbed glass show how the pitch varies in the S$_C^*$ phase : these drops are almost black between crossed polars, however they present fringes of equal thickness the contrast of which is very low. It is often useful, in order to make them visible, to insert a $\lambda/4$ plate before the analyzer ; their origin is an oscillation of the ellipticity of the transmitted light, the period of which is approximately half the pitch. The displacement of these fringes on the drop gives information on the variation of the pitch. In the case of $n = 10$, heating up the S$_C^*$ phase, one can clearly observe firstly a low increase of the pitch, next a sudden and important decrease, and immediately after filaments start to grow up and rapidly extend over the whole sample. The sudden decrease of the pitch is the signature of the S$_C^*$-S$_A$ transition. These observations thus confirm that the phase sequence is S$_C^*$-TGB$_A$ and that there is no TGB$_C$ phase.

The rotatory power of planar samples is important in the TGB$_A$ phase : for example 5°/μm for $\lambda = 546$ μm at 103.5 °C. Its values, in complete agreement with the De Vries law, confirms the pitch measurements (Δn is taken equal to 0.19 value measured in untwisted planar S$_A$ areas at the S$_C^*$-S$_A$ transition).

Figure 9b gives the pitch variations in the N* and TGB$_A$ phases of 11 F_2BTFO$_1$M$_7$. A noteworthy discontinuity is detected at the N*-TGB$_A$ transition (0.7 μm → 1 μm) : the Grandjean Cano threads are perfectly linear and their displacements are regular on cooling the N* phase ; they suddenly break apart at the N*-TGB$_A$ transition and next form, below this temperature, a new system of Grandjean Cano lines. We did not get correct measurements of the pitch divergence below 101 °C and in particular in the TGB$_C$ phase ; the reason is again a high viscosity that hinders the evacuation of the Grandjean lines. With the help of filaments appearing in drops with a pseudohomeotropic texture, we still observe the pitch divergence up to 10 μm at the TGB$_C$ → S$_C^*$ transition.

Furthermore, homeotropic drops deposited on rubbed glasses, presenting ellipticity fringes in the S$_C^*$ phase show on heating the following phenomenon : with a slow heating rate (< 1 °C.mn^{-1}) we first observe a weak increase of the pitch in the S$_C^*$ phase ; at 100 °C filaments appear and fill up the whole sample fairly rapidly ; no sudden pitch decrease preceeds the formation of filaments. This suggests that the S$_X^*$ phase that appears from the S$_C^*$ one is a TGB$_C$ phase. With a faster heating rate (~ 3 °C.mn^{-1}), filaments appear first and almost immediately after, in the S$_C^*$ homeotropic areas which are not yet invaded by the filaments, one clearly observes a drop of the S$_C^*$ pitch. This locates the A* phase at a higher temperature than the S$_C^*$-TGB$_C$ transition temperature, and confirms the S$_C^*$-TGB$_C$-TGB$_A$ sequence, the TGB$_C$ temperature range being very narrow. It is even possible to miss the formation of the TGB$_C$ phase (when the heating rate is too fast) : with 10 °C.mn^{-1} for instance, one clearly sees the sudden decrease of the S$_C^*$ pitch which points out the S$_C^*$-S$_A^*$ transition, a short time after the filaments develop in the homeotropic S$_A^*$.

Pitch measurements for the 12 F_2BTFO$_1$M$_7$ compound are reported in figure 9c. A discontinuity is detected at the N*-TGB$_C$ transition, its magnitude (0.44 μm → 1.5 μm) is larger than for $n = 11$. In the N* phase, measurements are performed by the Grandjean Cano method ; whereas in the TGB$_C$ phase the pitch is calculated from the rotatory power because

we did not manage to obtain regular Grandjean Cano steps in this phase. Below the N*-TGB_C transition the new system of lines refused to organize in steps. The first three values (at 103, 102.9 and 102.75 °C) are probably reliable. On the other hand, the values found for 102.6 and 102.2 °C are underrated ($P \simeq 2$ μm) : a high viscosity prevents the unwinding of the TGB_C phase. Pseudohomeotropic drops showing filaments allow a better evidence of the divergence of the pitch which grows up to 10 μm at the TGB_C-S_C^* transition. Furthermore, ellipticity fringes observed in homeotropic S_C^* drops reveal the absence of any pitch decrease, whatever the heating rate is ; this confirms the absence of any S_A phase and the sequence S_C^*-TGB_C-N*

7. Electrooptical properties.

We have studied the electrooptical properties of the S_C^* phase of 12 $F_2BTFO_1M_7$ in SSFLC configuration [18] including the temperature dependence of the response time, polarization and tilt angle. The sample thickness is around 3 μm (checked by Newton color method) the recurrence frequency is 3 KHz and the applied field corresponding to the saturation is around 30 V [19]. Figures 10, 11, 12 show, respectively, relatively high polarisation (about 50 nC/cm^2) quick response time (18 μs at 89 °C) and saturated tilt angle of 27°. These values

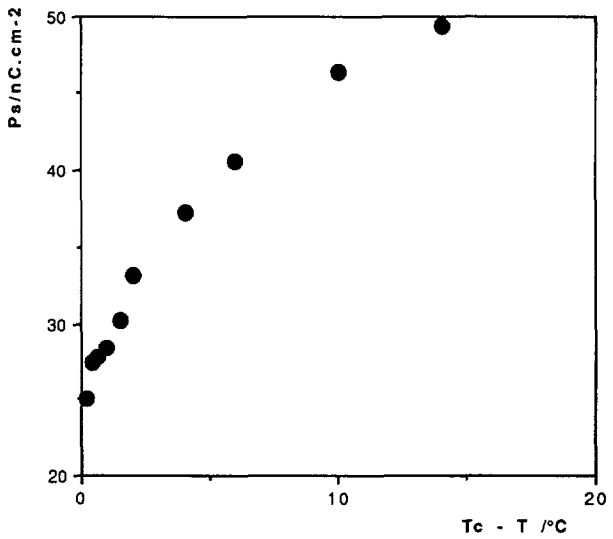

Fig. 10. — Spontaneous polarization of 12 $F_2BTO_2M_7$ *versus* $T_c - T$. The polarization current is induced by a square voltage (30 V, 3 kHz) applied on a 10 μm thick sample.

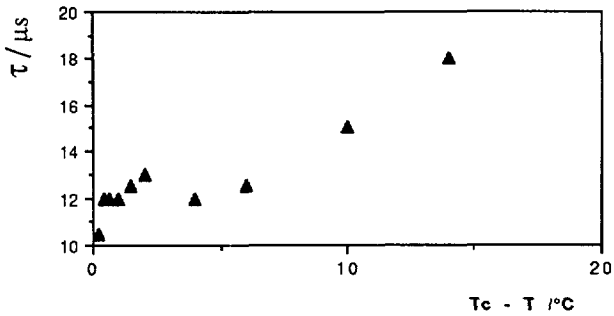

Fig. 11. — Response time *versus* $T_c - T$ ($f = 3$ kHz, $E = 30$ V).

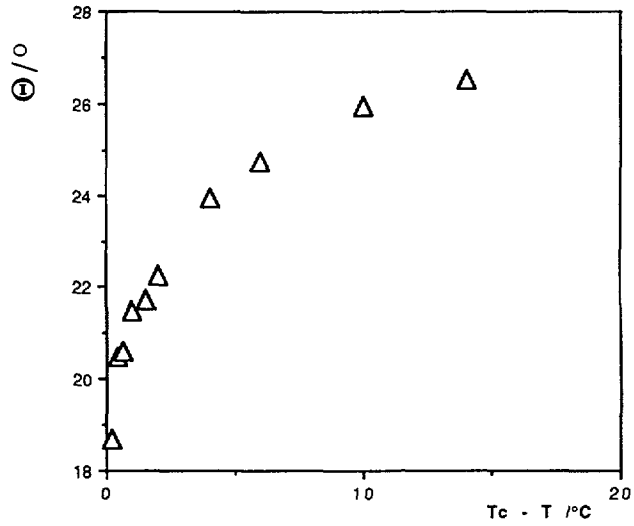

Fig. 12. — Tilt angle *versus* $T_c - T/(12\ F_2BTFO_1M_7)$.

are comparable with those obtained in the S_C^* phase of other compounds exhibiting a TGB$_A$ phase.

8. Discussion.

Since the discovery of the new helical smectic A* or TGB$_A$ phase in 1989 [1] several series have been published and some important parameters which have an influence on the formation of this new phase have been established for example the molecular polarity, especially the polarity near the chiral center, the optical purity and, of course, the nature of the chiral chains. We discuss here the role of the polarity near the core. It is well known that replacing the linking group -COO- between the chiral chain and the core by -O- with the same chiral chain (2-octanol) eliminates the S_A phase to the benefit of the cholesteric one. Indeed S_A is not observed with the linking group -O-. This tends to suggest that the S_A phase is favoured by the transverse polarity of the linking group. This remark was confirmed with the series obtained from -O- link and the chiral chains : 2-methylalkanoic acid or 2-(S), 3-(S)-2-chloro-3-methylpentanoic acid.

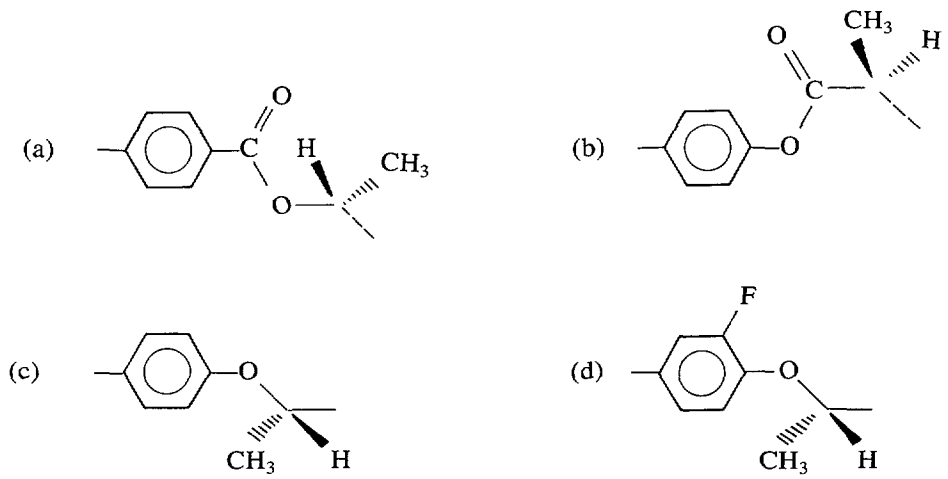

Let us consider now four situations a), b), c) and d) [20]. The molecules c) with a transverse electric dipole $\mu_\perp$ lower than the others (Tab. III) do not display the S_A phase and the phase sequence often observed is K-S_C^*-N* I whereas the molecules b) with a high $\mu_\perp$ = 1.54 D exhibit the S_A phase. Molecules b) and c) however do not present TGB phases. Table III shows that $\mu_\perp$ is nearly the same for molecules a) and b). The difference lies in the longitudinal dipole $\mu_\parallel$ which is respectively -0.63 and $+0.69$ for -$COOCH_3$ and -OOC-CH_3 because the former is an electron attractor group while the latter is a donor. The situation is more interesting with molecules d) which contain two different groups : F attractor and O-CH_3 (for instance) donor, the resulting longitudinal dipole $\mu_\parallel$ is : $-0.63 + 0.4 = -0.23$ D. So the combination of two groups F and OCH_3 is equivalent to an electron attractor group with $\mu_\parallel = -0.23$ D. In this latter case and with a chiral chain instead of -CH_3 for (OCH_3), we obtain not only a S_A phase but also TGB_A phase. We conclude that the formation of TGB phases is favoured by the presence of an electron attractor group linking the core to the chiral chain ($\mu_\parallel < 0$). A compromise must however be achieved : if $\mu_\parallel$ is too negative, S_A formation prevails over TGB_A stability. For example on molecules d) replacing F by CN or NO_2 groups generate S_A phases but not TGB phases.

Let us point out the interesting effect of fluorine on molecules d) [20]. Beside the attractor effect, fluorine has also a steric hindrance effect which favours the formation of tilted phases and in this case the TGB_C phase.

Table III. — *Dipolar moments (D) and angles (°) of group* X *attached to* C_6H_5-.

Group X	μ (D)*	$\mu_\perp$ (D)*	$\mu_\parallel$ (D)*	θ (°)**
-OCH_3	+ 1.28	1.2	+ 0.4	72
-$OCOCH_3$	+ 1.69	1.54	+ 0.69	66
-$COOCH_3$	− 1.85	1.7	− 0.63	110
-F	− 1.47	1.27•	− 0.63•	—

* The positive sign is taken for groups X that are positive poles of the dipole C_6H_5-X (donor group).

** The angle θ is defined in the following way : C_6H_5-$\theta\lambda$ X . $\theta < 0°$ for X donors.

• Calculated for example in situation (*d*) of the molecule.

9. Conclusion.

We believe that the new helical phase S_X^* we have discovered in the $n = 11$ and $n = 12$ homologs of the series $nF_2BTFO_1M_7$ is a good candidate for the tilted twist grain boundary (TGB_C) structure predicted by Renn and Lubensky [5] and Renn [15] for the following reasons :

(i) X-ray diffraction studies on powder samples show long range correlations of the smectic layers for $n = 10$ and $n = 12$ ($\xi > 6\,000$ Å) in both S_A^* and S_X^* phases.

(ii) The macroscopic helical structure is demonstrated by pitch measurements on oriented samples (Sect. 6). The observation of the same system of Grandjean-Cano lines in the cholesteric, S_A^* and S_X^* phases with planar alignment conditions shows that the helical axis is

essentially perpendicular to the glass walls in the three structure whereas it flips to lie parallel to the walls in the S_C^* phase. This observation suggests that the helical axis is perpendicular to the director in both S_X^* and S_A^* phases.

(iii) Both S_A^* and S_X^* phases disappear to the benefit of S_A and S_C respectively when the molecular chirality is turned off by mixing (R) and (S) enantiomers (see Sect. 4).

(iv) The tilt of the director relative to the layer normal in the S_X^* phase only (i.e. smectic C like local order) is inferred from two independent observations :

- a sharp but continuous decrease of the layer spacing upon cooling from the non tilted S_A^* phase ($n = 11$ homolog) and from the cholesteric phase with short range smectic C order ($n = 12$) ;
- a noticeable tilt angle (18.5°) measured in the S_C^* phase of the $n = 12$ homolog at the $S_X^* - S_C^*$ transition while no significant change of the layer spacing is detected at this transition.

Points (i) to (iii) suggest of course that S_A^* is a TGB$_A$ phase. If these two identifications are accepted, the experimental phase diagram of figure 5 appears to have the same topology as the theoretical phase diagram of Renn [15] (Fig. 1). The line TGB$_A$-S_C^* is found between pure 10 F_2BTFO$_1$M$_7$ and ~ 35 % 11 F_2BTFO$_1$M$_7$. The TGB$_A$-TGB$_C$-S_C^* point B_3 is found (~ 35 % $n = 11$ in $n = 10$). Although we could not locate it accurately the N*-TGB$_A$-TGB$_C$ (L) point is present in the ($n = 11$, $n = 12$) mixture.

The phase sequences of other homologs (not presented here) show in fact that two other remarkable points of the theoretical diagram exist in the same series nF$_2$BTFO$_1$M$_7$. The TGB$_A$-S$_A$-S_C^* point B_2 lies in between the $n = 9$ and $n = 10$ homologs : whereas the $n = 14$ derivative presents a direct transition N*-S_C^* showing that the N*-TGB$_C$-S_C^* point exists in a binary mixture somewhere in between $n = 12$ and $n = 14$. Investigation of the complete phase diagram is currently in progress.

We confirm that the TGB$_A$-S_C^* and TGB$_C$-S_C^* are first order : DSC data do show a transition enthalpy and thermal hysteresis whereas the helical pitch is discontinuous. A weak transition enthalpy is however also detected at the TGB$_A$-TGB$_C$ transition which we believe is weakly first order. The broad peak associated with the small N*-TGB$_A$ transitions reveals strong pretransitional effects but we cannot distinguish a second order from a weakly first order transition. The TGB$_C$-S_C^* transition is not detected from the variations of the layer spacing d with temperature which supports the theoretical prediction that the tilt angle of the TGB$_C$ phase is very close to the bulk smectic C tilt angle.

No evidence of a possible TGB$_{C*}$ phase was found.

We would like to point out an interesting property that we expect from the TGB$_C$ phase : each smectic C slab of the TGB$_C$ structure is made of chiral molecules and therefore bears a non zero electric polarization as shown by Meyer *et al.* [18] in 1975. If the director lies in the plane perpendicular to the pitch axis as argued by Renn and Lubensky [5] and Renn [15], the polarization $\mathbf{p}_i$ of each slab lies parallel to the pitch axis. Furthermore, if the projection $\mathbf{c}$ of the director on the layer plane points towards the same side of the layer normal in the neighbouring slabs (ferromagnetic stack of slabs, see Ref. [15]) the polarizations $\mathbf{p}_i$ add up and the TGB$_C$ phase is ferroelectric [22]. Unlike the helielectric S_C^*, the TGB$_C$ structure described by Renn and Lubensky [5] and Renn [15] ought to be truly ferroelectric with a permanent polarization along the pitch axis. Note that a tilt of the director along the pitch axis in the smectic C slabs would produce a helical polarization instead. Such a helielectric TGB$_C$ structure would cost more electric energy as argued by Renn and Lubensky but presumably less electrostatic energy. Experimental study of the effect of an electric field on the TGB$_C$ structure is currently in progress.

Finally, coming back to the molecular level, we would like to emphasize the interesting

conclusion that a chemical characteristics of the molecules exhibiting TGB phases seem to emerge from the limited, but increasing number of experimental observations : a moderately strong electron attractor link between the core and the chiral chain clearly favours the formation of TGB structures. This remark should help chemical synthesis in the search of new material exhibiting the fascinating TGB smectic phases.

Acknowledgments.

The authors would like to thank E. Frossard for her help in preparing surface oriented samples.

References

[1] GOODBY J. W., WAUGH M. A., STEIN S. M., CHIN E., PINDAK R. and PATEL J. S., *Nature* (London) **337** (1989) 449.
[2] GOODBY J. W., WAUGH M. A., STEIN S. M., CHIN E., PINDAK R. and PATEL J. S., *J. Am. Chem. Soc.* **111** (1989) 8119.
[3] SRAJER G., PINDAK R., WAUGH M. A., GOODBY J. W. and PATEL J. S., *Phys. Rev. Lett.* **64** (1990) 13.
[4] RENN S. R. and LUBENSKY T. C., *Phys. Rev. A* **38** (1988) 2132.
[5] RENN S. R. and LUBENSKY T. C., *Mol. Cryst. Liq. Cryst.* **209** (1991) 349.
[6] LAVRENTOVICH O. D., NASTISHIN Y. A., KULISHOV V. I., NARKEVICH Y. S., TOLOCHKO A. S. and SHIYANOVSKII S. V., *Europhys. Lett.* **13** (1990) 313.
[7] SLANEY A. J. and GOODBY J. W., *J. Mat. Chem.* **1** (1991) 5.
[8] SLANEY A. J. and GOODBY J. W., *Liq. Cryst.* **9** (1991) 849.
[9] NGUYEN H. T., TWIEG R. J., NABOR M. F., ISAERT N. and DESTRADE C., *Ferroelectrics* **121** (1991) 187.
[10] BOUTCHA A., NGUYEN H. T., ACHARD M. F., HARDOUIN F., DESTRADE C., TWIEG R. J., MAAROUFI A. and ISAERT N., *Liq. Cryst.*, under press.
[11] FREIDZON Y. S., TROPSHA Y. G., TSUKRUK V. V., SHILOV V. V., SHIBAEV V. P. and LIPATOV Y. S., *J. Polym. Chem. (USSR)* **29** (1987) 1371.
[12] BUNNING T. J., KLEI H. E., SAMULSKI E. T., CRANE R. L. and LINVILLE R. J., *Liq. Cryst.* **10** (1991) 445.
[13] GILLI J. M. and KAMAYE M., *Liq. Cryst.* **11** (1992) 569.
[14] DE GENNES P. G., *Solid State Commun.* **10** (1972) 753.
[15] NABOR M. F., NGUYEN H. T., DESTRADE C., MARCEROU J. P. and TWIEG R. J., *Liq. Cryst.* **10** (1991) 785.
[16] RENN S. R., *Phys. Rev. A* **45** (1992) 953.
[17] KELLY S. M., *Helv. Chim. Acta* **72** (1989) 594.
[18] CLARK N. A. and LAGERWALL S. T., *Appl. Phys. Lett.* **36** (1980) 899.
[19] CHEN J. and LUBENSKY T. C., *Phys. Rev. A* **14** (1976) 1202.
[20] FURUKAWA K., TERASHIMA K., ICHIHASKI M., SAITOH S., MIYAZAWA K. and INUKAI T., *Ferroelectrics* **85** (1988) 451.
[21] MINKIN V. I., OSIPOV O. A., ZHDANOV Yu A., Dipole moments in Organic Chemistry (Plenum Press, 1970).
[22] The ferroelectricity of the TGB_C structure was also mentionned to us by S. Renn in a private communication.